Letter

A new solar spectral selective absorbing coating of SS–(Fe$_3$O$_4$)/Mo/ TiZrN/TiZrON/SiON for high temperature application

Yu Liu [a,b], Zhifeng Wang [a], Dongqiang Lei [a], Cong Wang [b,*]

[a] Key Laboratory of Solar Thermal Energy and Photovoltaic System, Institute of Electrical Engineering, Chinese Academy of Sciences, Beijing 100190, PR China
[b] Center for Condensed Matter and Materials Physics and Key Laboratory of Micro–nano Measurement, Manipulation and Physics (Ministry of Education), Department of Physics, Beihang University, Beijing 100191, PR China

A B S T R A C T

In this study, a solar spectral selective absorbing coating of SS–(Fe$_3$O$_4$)/Mo/TiZrN/TiZrON/SiON exhibiting an absorptance of 0.95 and an emittance of 0.08 at 80 °C is reported. The structure and morphology of each layer were investigated by X-ray and Fourier transform infrared spectroscopic analyses. After heat treatment at 500 °C for 300 h in vacuum, the values of absorptance and emittance became 0.92 and 0.10 (at 80 °C), respectively. Moreover root mean square roughness of the coating measured by atomic force microscopy increased to 8.14 nm from 4.79 nm, indicating good thermal stability at 500 °C.

© 2014 Elsevier B.V. All rights reserved.

1. Introduction

In recent years, less expensive transition metal/transition metal alloy nitride/nitro-oxides, such as NbN, TiON, and TiMON (M represents metal), have attracted significant attention as stable absorbing layer in high-temperature solar selective absorbing coatings for parabolic trough concentrated solar power (CSP) photo-thermal conversion [1–5]. Highly absorbing metal–dielectric composite coatings, or cermet, consist of fine metal particles in a dielectric or ceramic matrix. However, fine metal particles can easily diffuse, congregate, or oxidize, in particular, in high temperature applications [6]. It causes deterioration in the optical properties of the coating at high temperature. Extensive research efforts have been devoted to binary or ternary transition metal alloy nitride/nitro-oxides because of their efficient performance in diffusion barrier and high temperature oxidation resistance [7–10]. Panjan et al. [9] showed that the oxidation resistance of both Cr$_{0.72}$Ti$_{0.28}$N and TiN/CrN multilayer coatings was better than that of single CrN or TiN layers, respectively. Previously, we reported Nb–NbN solar selective absorbing coating with good spectral selectivity and thermal stability [2]. For further improving the high temperature stability, NbTiON solar selective absorbing coating with high absorptance (0.95), low emittance (0.07), and good thermal stability at 500 °C in vacuum was deposited [3]. In this

study, NbTi alloy was substituted by TiZr to design a coating with the following film structure: SS–(Fe$_3$O$_4$)/Mo/TiZrN/TiZrON/SiON. SS–(Fe$_3$O$_4$) is the substrate with surface oxidation (Fe$_3$O$_4$) of stainless steel (SS) piece. The Mo layer acted as infrared reflective layer and SiON layer acted as the antireflective layer. The TiZrN and TiZrON layers acted as double absorbing layers. Moreover, the TiZrN layer acted as diffusion barrier between SS substrate and absorbing layer. The TiZrON layer incorporating TiZrN layer played a significant role in the destructive interference to enhance absorbance. In practice, it has been reported that TiZrN, TiN, and ZrN films have high hardness, high thermal and chemical stability, and low electrical resistivity [10–12]. In this study, the spectral properties (absorptance and emittance), microstructure, and thermal stability of SS–(Fe$_3$O$_4$)/Mo/TiZrN/TiZrON/SiON coating were investigated.

2. Experiment details

The coating was deposited on SS substrates (dimensions 30 mm × 30 mm) by a JGP350C reactive DC/RF magnetron sputtering system with multi-target arrangement. The SS substrates were heated in air at 700 °C for 30 min to produce Fe$_3$O$_4$ layer after cleaning to avoid interface diffusion between SS and Mo layers by oxidation of the substrate surface. The purity, diameter and thickness of the Mo, TiZr and SiN targets are 99.99%, 60 mm and 4 mm, respectively. The infrared reflective Mo layer was deposited by a DC magnetron sputtering method. TiZrN and TiZrON layers

* Corresponding author. Tel./fax: +86 10 82338346.
E-mail address: congwang@buaa.edu.cn (C. Wang).

Table 1
The absorptance, emittance and solar spectral selectivity (α/ε) of the layer-added film samples before and after heat-treatment at 500 °C.

Samples	Solar spectral selectivity α/ε		
	As-deposited	Annealed	$\Delta\alpha/\Delta\varepsilon$
SS substrate	0.36/0.10 = 3.6	–	–
SS–(Fe$_3$O$_4$)	0.72/0.14 = 5.1	–	–
SS–(Fe$_3$O$_4$)/Mo	0.45/0.05 = 9	–	–
SS(Fe$_3$O$_4$)/Mo/TiZrN	0.77/0.08 = 9.6	–	–
SS(Fe$_3$O$_4$)/Mo/TiZrN/TiZrON	0.85/0.08 = 10.6	–	–
SS(Fe$_3$O$_4$)/Mo/TiZrN/TiZrON/SiON	0.95/0.08 = 11.8	0.93/0.08 (80 h)	−0.02/0
		0.92/0.10 (300 h)	−0.03/0.02

were deposited at room temperature using Ti–Zr (1:1, at%) alloy target with different O$_2$/N$_2$ gas flow rates by DC magnetron sputtering. The TiZrN layer was deposited at a nitrogen flow rate of 10 sccm. For TiZrON layer, the flow rates for O$_2$ and N$_2$ gases were 5 and 10 sccm, respectively. SiON layer was deposited using RF power with SiN target at the O$_2$/N$_2$ gas flowing rate of 1/10. The sputtering pressure and flow rate of argon gas were kept constant for all the layers, at 0.5 Pa and 80 sccm, respectively.

The reflective spectra $R(\lambda)$ were measured by a UVPC3100 spectrophotometer in the wavelength range of 0.2–2.6 µm and Bruker Tensor 27 spectrometer in the range of 2.6–25 µm. The UVPC3100 was equipped with an integrating sphere coated with barium sulfate; this instrument is divided into two spectral ranges from 0.2 to 0.8 and 0.8 to 2.6 µm with the source of deuterium and tungsten lamps. The Bruker Tensor 27 is a type of Fourier Transform Infrared Reflectance (FTIR) spectrometer equipped with an integrating sphere coated with gold. The total solar absorptance (α_s) calculated with a normal angle of incidence is a weighted average, obtained by using the solar spectral radiation ($I_s(\lambda, T)$), as shown in the following equation:

$$\alpha_s = \frac{\int_{\lambda_1 = 0.3}^{\lambda_2 = 2.5} (1 - R(\lambda)) I_s(\lambda) d\lambda}{\int_{\lambda_1 = 0.3}^{\lambda_2 = 2.5} I_s(\lambda) d\lambda} \qquad (1)$$

where $R(\lambda)$ is the measured reflectance at a specific wavelength λ, and $I_s(\lambda)$ is the solar spectra irradiation. The nearly normal emittance was measured by a NEM-80 normal emittance tester at 80 °C, a normal emissivity measuring instrument based on comparing between sample's radiation and blackbody's radiation at the same temperature (80 °C) to obtain the normal emittance of the sample [13]. Absorptance and emittance depend on the operating temperature. The solar absorptivity is expected to change a little at higher temperatures. In contrast, the thermal emissivity at different temperatures is strongly dependent on the position and sharpness of the cut-off edge from low reflectivity to high reflectivity at the operating temperature:

$$\varepsilon_t = \frac{\int_{\lambda_3 = 0.3}^{\lambda_4 = 100} (1 - R(\lambda)) I_b(\lambda, T) d\lambda}{\int_{\lambda_3 = 0.3}^{\lambda_4 = 100} I_b(\lambda, T) d\lambda}$$

For the measurement of thickness, first the deposition rate was obtained by preparing a thick single layer separately and measuring the thickness by a VEECO dektak 6M type α-step profilometer. Finally, the thickness of each layer in the multilayer films was determined by the deposition rate and deposition time. The phase formation and crystal structure of the films were determined by X-ray diffraction (XRD) analysis using a Dmax diffractometer. The AVATAR Fourier Transform Infrared spectroscopy (FTIR) was used to characterize the composition of amorphous SiON layer. Surface images of the as-deposited and annealed samples were obtained using AFM (CSPM400, BenYuan Ltd.) in the contact mode. To test

the thermal stability, the coatings deposited on SS substrates were heated twice at 500 °C for a long period in vacuum.

3. Results and discussion

3.1. Spectral properties

The absorptance, emittance and solar selectivity values for the layer-added films of SS–(Fe$_3$O$_4$), SS–(Fe$_3$O$_4$)/Mo, SS–(Fe$_3$O$_4$)/Mo/TiZrN, SS–(Fe$_3$O$_4$)/Mo/TiZrN/TiZrON and SS–(Fe$_3$O$_4$)Mo/TiZrN/TiZrON/SiON are listed in Table 1. Results obtained using SS substrate are provided for comparison. The SS–(Fe$_3$O$_4$)/Mo/TiZrN/TiZrON/SiON coating exhibited a high absorptance (α) of 0.95 and a low emittance (ε) of 0.08. The method employed for optimization of the double absorbing layers (TiZrN and TiZrON) was similar to that for the two NbTiON sublayers [3].The thickness of Mo and antireflective layers was obtained from previous studies [3,14]. The optimized thicknesses of Mo, TiZrN, TiZrON, and SiON layers were 200, 100, 30 and 65 nm, respectively. The solar radiation was mainly absorbed through two methods: intrinsic absorption and interference absorption. The TiZrN absorbing layer provided the maximum contribution to the absorbance through intrinsic absorption; however, it led to an increase in the emittance. The destructive interference between TiZrN and TiZrON layers led to a further increase in absorbance. Moreover, presence of the SiON layer further increased the solar absorbance due to the antireflective effect. The Mo infrared reflective metal layer exhibited a low emittance of 0.05. The reflective spectra of the layer-added film samples are shown in Fig. 1, and the results correspond to the data listed in Table 1.

3.2. Structural characterization

XRD and FTIR analyses were used to determine the phase structure of each layer. Fig. 2a shows the peaks corresponding to SS–(Fe,C), Fe$_3$O$_4$ and Mo in SS–(Fe$_3$O$_4$)/Mo. A 500 nm thick TiZrN layer was deposited on a glass substrate for XRD analysis. The peaks corresponding to TiN and Zr$_2$N are observed in the XRD pattern (Fig. 2b) indicating that the obtained TiZrN layer consists of TiN and Zr$_2$N phases. Therefore, it can be assumed that the TiZrN layer is a mixture of TiN and Zr$_2$N aiding in diffusion barrier application [11].

The TiZrON and SiON layers did not exhibit any XRD peak, indicating their amorphous nature. A 350 nm thick SiON layer was deposited on Si substrate to comply with the FTIR characterization. Fig. 3 shows the superposition and fitting of the FTIR spectrum of the SiON layer. The strongest absorption peaks at 1060 cm^{-1} and 890 cm^{-1} are attributed to Si–O in SiO$_2$ and Si–N in Si$_3$N$_4$, respectively [15]. Therefore, the presence of SiO$_2$ and Si$_3$N$_4$ phases could be suspected, even in the case of amorphous structure.
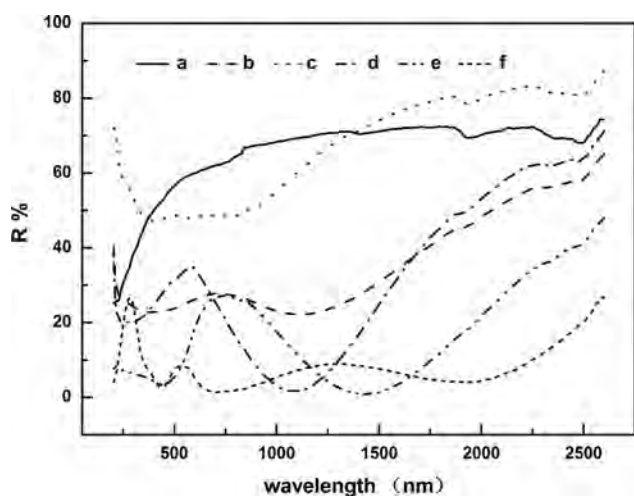
Fig. 1. The reflective spectra of the layer-added coating samples of (a) SS substrate, (b) SS–(Fe$_3$O$_4$), (c) SS–(Fe$_3$O$_4$)/Mo, (d) SS–(Fe$_3$O$_4$)/Mo/TiZrN, (e) SS–(Fe$_3$O$_4$)/Mo/TiZrN/TiZrON, and (f) SS–(Fe$_3$O$_4$)Mo/TiZrN/TiZrON/SiON.
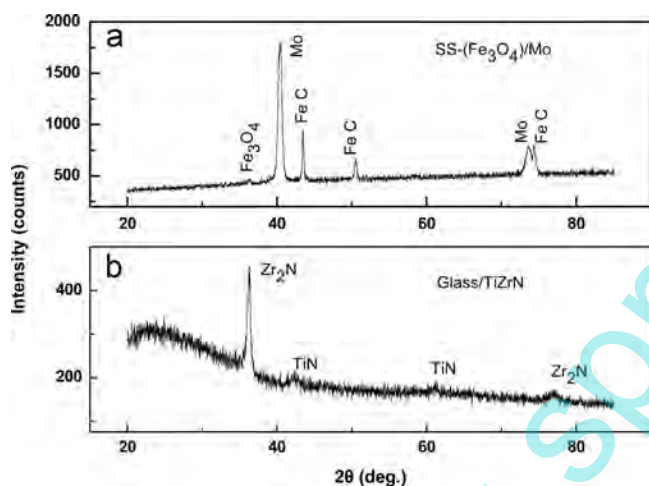
Fig. 2. XRD patterns of (a) SS–(Fe$_3$O$_4$)/Mo and (b) TiZrN layer on glass substrate.

Fig. 3. The superposition and fitting of the FTIR absorption spectrum of the SiON layer, indicating the presence of distinct SiO$_2$ and Si$_3$N$_4$ phases.

Fig. 4. The reflective spectra of SS–(Fe$_3$O$_4$)/Mo/TiZrN/TiZrON/SiON before and after heat treatment in the range of 0.2–25 μm at 500 °C.

3.3. Thermal stability

The high temperature stability of the solar selective absorbing coatings is extremely significant at 400 °C or higher for long periods, for high temperature application in parabolic trough CSP. [14] The thickness of the entire coating was determined to be 400 nm. The phase structural and interface structural stability of the coating with the total thickness of less than 1.0 μm is essential for the permanence of the spectral selectivity, which determines the lifetime of the coatings in applications.

The coating samples were kept in a quartz tube with the vacuum of 5×10^{-1} Pa, heated up to 500 °C, and finally maintained at the desired temperature for 40 h. After being cooled down to room temperature, the samples were again immediately heated up to 500 °C for 40 h. Finally, the samples were heated up to 500 °C for 300 h. Later, the spectral properties of the annealed samples were measured. The absence of significant changes in the values of absorptance and emittance indicated good thermal stability of the coating at that temperature.

Comparison of the values of absorptance and emittance of the coating before and after heat-treatment is presented in Table 1. Insignificant changes are observed in the values of absorptance a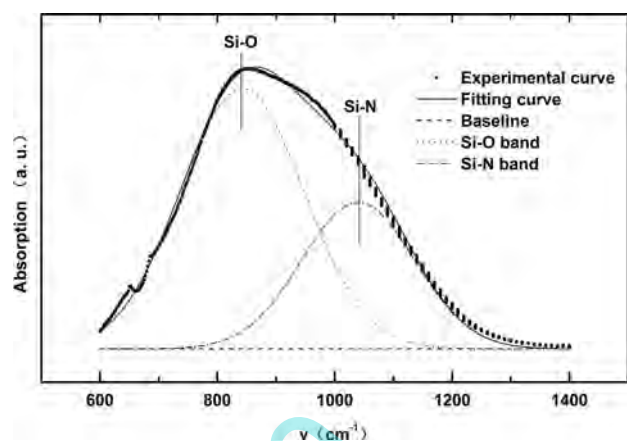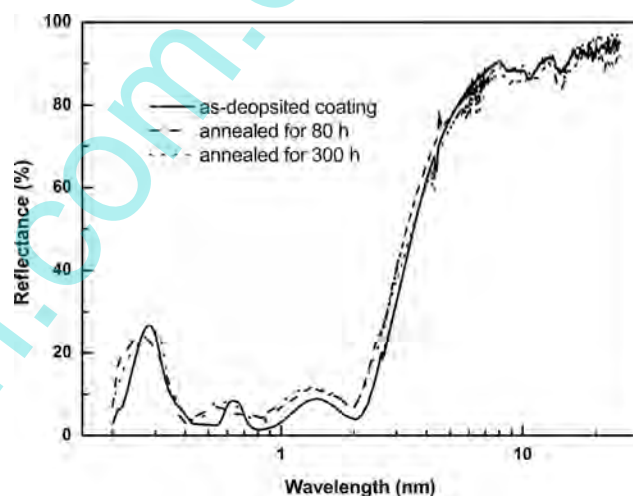nd emittance. Reflective spectra shown in Fig. 4 confirm the above mentioned results and display increase in the reflectivity in the range of 0.5–25 μm for the annealed coating.

Fig. 5 shows three-dimensional AFM images of the SS–(Fe$_3$O$_4$)/Mo/TiZrN/TiZrON/SiON coating before and after heat treatment. The as-deposited coating exhibits a root mean square (RMS) roughness of 4.79 nm [16] (Fig. 5) and shows a columnar microstructure with a textured surface, as expected for the sputtered coatings grown from the vapor phase at low temperature. The obtained columnar structure with surface texture could increase light absorption, thus increasing solar absorption and thermal stability [17]. Fig. 5b demonstrates an insignificant increase in the RMS roughness when the coating was annealed at 500 °C (5.23 nm (80 h) and 8.14 nm (300 h)). Emittance from the surface provides considerable contribution and depends on the condition of the material surface, including the surface microstructure, morphology, roughness, and the surface oxide layers [18,19]. Negligible change in RMS roughness was observed after annealing and significant increase in emittance was not observed. The above mentioned results indicated that the SS–(Fe$_3$O$_4$)/Mo/TiZrN/TiZrON/SiON coating was thermally stable at 500 °C in vacuum.

High temperature heat-treatment could induce microstructure degradation such as inter-diffusion and reaction at the interface resulting in phase decomposition, transformation, and oxidation, as investigated in our previous work [3]. The oxidation and diffusion of NbTiON into the Cu substrate resulted in degradation
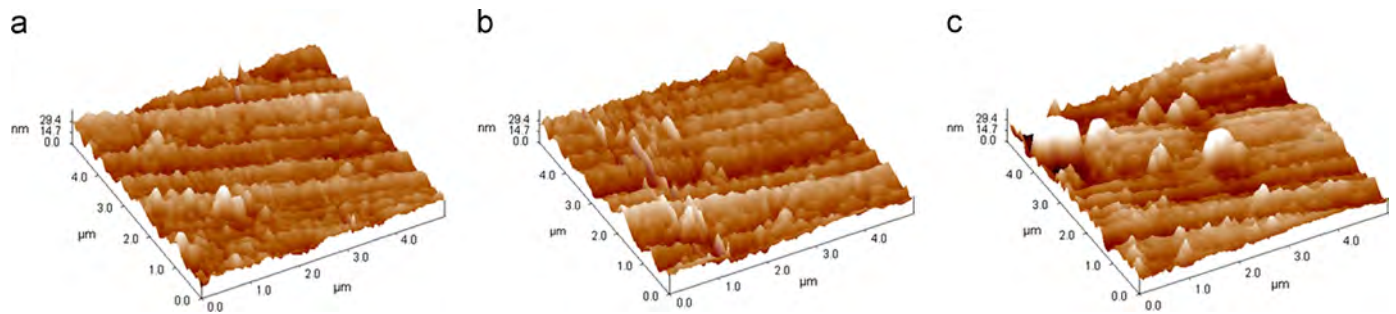
Fig. 5. Three dimensional AFM images of the coatings: (a) as-deposited, (b) heat-treated at 500 °C for 80 h, and (c) heat–treated at 500 °C for 300 h.

of the NbTiON solar selective absorbing coating. In the case of SS–(Fe_3O_4)/Mo/TiZrN/TiZrON/SiON coating, Fe_3O_4, acting as a diffusion barrier in the interface of Mo layer and SS substrate, has been reported to effectively hold back the occurrence of the complex phases such as Mo_2C and Fe_2MoC which are responsible for increasing emissivity [2]. The TiZrN layer composed of TiN and Zr_2N phases is believed to be highly oxidation resistant and good diffusion barrier, indicating a minimal diffusion between the layers. In the reported Cu/TiZrN/Si contact system [11], a TiZrN film with $\sim$10 nm thickness acted as the barrier, adequate to suppress the penetration of extremely small quantity of Cu into the Si substrate upon annealing at 600 °C for 1 h without significant structural changes and solid-phase reaction. Moreover the strong oxidation-resistant ability of the SiON layer on the upper surface could suppress oxygen diffusion, thus reducing the oxidation rate of the entire coating [13,20].

4. Conclusion

In this study, a solar selective absorbing coating with the film structure of SS–(Fe_3O_4)/Mo/TiZrN/TiZrON/SiON was developed which exhibited high absorptance of 0.95 and low emittance of 0.08. XRD analysis indicated that the prepared TiZrN layer consisted of TiN and Zr_2N phases, and the SiON and TiZrON layers were amorphous in nature. After heat-treatment at 500 °C for 300 h in vacuum, the absorptance and emittance values of the coating became 0.92 and 0.10, respectively. No significant change was found in RMS roughness, as confirmed by AFM measurements, indicating good thermal stability at 500 °C. The coating exhibited significant potential as solar selective absorbing surface for high-temperature photo-thermal conversion in CSP applications.

Acknowledgement

References

[1] A. Biswas, D. Bhattacharyya, H.C. Barshilia, N. Selvakumar, K.S. Rajam, Appl. Surf. Sci. 254 (2008) 1694–1699.
[2] Du Xinkang, Wang Tianmin, Wang Cong, Chen Buliang, Zhou Long, Chin. J. Aeronaut. 20 (2007) 140–144.
[3] Yu Liu, Cong Wang, Yafei Xue, Sol. Energy Mater. Sol. Cells 96 (2012) 131–136.
[4] Dechun Zhu, Fang Mao, Shuxi Zhao, Sol. Energy Mater. Sol. Cells 98 (2012) 179–184.
[5] J.B. Metson, K.E. Prince, A. Bittar, L.J. Tornquist, Ionics 7 (2001) 346–350.
[6] C.E. Kennedy, National Renewable Energy Laboratory of USA, 2002 (Technical report).
[7] Liu Aiqin, Sun Lu, Li Shusuo, Han Yafang, J. Rare Earths 25 (2007) 474–479.
[8] A.K. Vasudevan, J.J. Petrovic, Mater. Sci. Eng. 155 (1992) 1–17.
[9] P. Panjan, B. Navinšek, A. Cvelbar, A. Zalar, I. Milošev, Thin Solid Films 281–282 (1996) 298–301.
[10] Roland Hauert, Jorg Patscheider, Adv. Eng. Mater. 2 (2000) 247–259.
[11] Mayumi B. Takeyama, Takaomi Itoi, Eiji Aoyagi, Atsushi Noya, Appl. Surf. Sci. 216 (2003) 181–186.
[12] A. Hoerling, J. Sjolén, H. Willmann, T. Larsson, M. Odén, L. Hultman, Thin Solid Films 516 (2008) 6421–6431.
[13] Yin Zhiqiang, Yan xiyuan, Chen Tenghua, Zhao Tiesong, An Ruhong, Tang Xuan, Acta Energiae Solaris Sin. 17 (1996) 50–55.
[14] Du Xinkang, Wang Cong, Wang Tianmin, Zhou Long, Chen Buliang, Ru Ning, Thin Solid Films 516 (2008) 3971–3977.
[15] F. Rebib, E. Tomasella, M. Dubois, J. Cellier, T. Sauvage, M. Jacquet, Thin Solid Films 515 (2007) 3480–3487.
[16] Ashwini Kumar Singh, Neelam Kumari, S.K. Mukherjee, P.K. Barhai, Int. J. Res. Rev. Appl. Sci. 14 (2013) 603–611.
[17] V. Teixeira, E. Sousa, M.F. Costa, C. Nunes, L. Rosa, M.J. Carvalho, M. Collares-Pereira, E. Roman, J. Gago, Thin Solid Films 392 (2001) 320–326.
[18] C.G. Granqvist, Appl. Phys. A 52 (1991) 83–93.
[19] B.O. Seraphin, Topics in Applied Physics, 31, Springer, Berlin, 1979.
[20] R.K. Pandey, L.S. Patil, J.P. Bange, D.R. Patil, A.M. Mahajan, D.S. Patil, D.K. Gautam, Opt. Mater. 25 (2004) 1–7.